Two-Photon Fluorescence Microscopy of Laurdan Generalized Polarization Domains in Model and Natural Membranes

Tiziana Parasassi,* Enrico Gratton,# Weiming M. Yu,# Paul Wilson,§ and Moshe Levi§

*Istituto di Medicina Sperimentale, CNR, Rome, Italy; #Laboratory for Fluorescence Dynamics, University of Illinois at Urbana-Champaign, Urbana, Illinois, USA; and §The University of Texas Southwestern Medical Center at Dallas and Department of Veterans Affairs Medical Center, Dallas, Texas 75216 USA

ABSTRACT Two-photon excitation microscopy shows coexisting regions of different generalized polarization (GP) in phospholipid vesicles, in red blood cells, in a renal tubular cell line, and in purified renal brushborder and basolateral membranes labeled with the fluorescent probe laurdan. The GP function measures the relative water content of the membrane. In the present study we discuss images obtained with polarized laser excitation, which selects different molecular orientations of the lipid bilayer corresponding to different spatial regions. The GP distribution in the gel-phase vesicles is relatively narrow, whereas the GP distribution in the liquid-crystalline phase vesicles (DOPC and DLPC) is broad. Analysis of images obtained with polarized excitation of the liquid-crystalline phase vesicles leads to the conclusion that coexisting regions of different GP must have dimensions smaller than the microscope resolution (~200 nm radially and 600 nm axially). Vesicles of an equimolar mixture of DOPC and DPPC show coexisting rigid and fluid domains (high GP and low GP), but the rigid domains, which are preferentially excited by polarized light, have GP values lower than the pure gel-phase domains. Cholesterol strongly modifies the domain morphology. In the presence of 30 mol% cholesterol, the broad GP distribution of the DOPC/DPPC equimolar sample becomes narrower. The sample is still very heterogeneous, as demonstrated by the separations of GP disjoined regions, which are the result of photoselection of regions of different lipid orientation. In intact red blood cells, microscopic regions of different GP can be resolved, whereas in the renal cells GP domains have dimensions smaller than the microscope resolution. Preparations of renal apical brush border membranes and basolateral membranes show well-resolved GP domains, which may result from a different local orientation, or the domains may reflect a real heterogeneity of these membranes.

INTRODUCTION

Lipids in biomembranes are the milieu for boundary functions of cells, including stimuli to growth and to immunological and stress response, i.e., information delivered from the environment to the cell interior. Membranes of internal organelles allow the compartmentalization of cell functions. Extensive literature exists on the influence of the membrane lipid dynamics on all of the above cell functions (Aloia et al., 1993; Grant, 1983; Maresca and Cossins, 1993). In particular, given the complexity of the membrane lipid composition, questions have been raised with regard to the possible coexistence of domains of different dynamical properties in the membrane plane, these domains being of relevance for a putative preferential partitioning of proteins and of solutes, for modulating membrane activity, and for diffusion along the plane and through the bilayer.

Fluorescence spectroscopy is one of the commonly used tools for the investigation of lipid dynamical properties. The information on membrane packing and dynamics is obtained from spectroscopic properties such as excitation and emission spectra, polarization, and lifetime of fluorescent probes in the membrane. Among several fluorescent probes, the sensitivity of 2-dimethylamino-6-lauroylnaphthalene (laurdan) to the polarity of its environment has presented several advantages for membrane studies. This probe shows spectral sensitivity to the polarity of its environment, with a 50-nm red shift of its emission maximum in polar versus nonpolar environments, so that simple fluorescence intensity measurements at two properly selected wavelengths provide information on the membrane polarity. Several studies have shown that laurdan spectroscopic properties reflect local water content in the membrane (Parasassi and Gratton, 1995). Also, for laurdan, a modification of the ratiometric method was previously developed, the generalized polarization (GP) function, which allows rapid and fine measurements of the emission spectral shift (Parasassi et al., 1990). Laurdan was thus an ideal candidate for microscopy measurements, but its use was limited because of its rapid fading. Only recently has the development of the two-photon fluorescence microscopy made it possible to minimize photobleaching problems.

In "cuvette studies," the dependence of the GP value on the excitation wavelength has been used to discriminate between membranes composed of a homogeneous phase and of coexisting domains of gel and liquid-crystalline phases. Excitation GP spectra are calculated by reporting the GP value as a function of the excitation wavelength, i.e., the GP value defined as $GP = (I_{440} - I_{490})/(I_{440} + I_{490})$ as a function of the excitation wavelength. For model membrane systems labeled with laurdan, a negative slope of the GP excitation spectrum indicated a homogeneous liquid-

Received for publication 18 October 1996 and in final form 11 February 1997.

Address reprint requests to Dr. Moshe Levi, 4500 South Lancaster Road, 151 Dallas, TX 75216. Tel.: 214-376-5451, ext. 5526 or 5580; Fax: 214-372-7948; E-mail: mmjjl@aol.com.

0006-3495/97/06/2413/17 $2.00

crystalline environment, and a positive slope indicated the coexistence of gel and liquid-crystalline phase domains (Parasassi and Gratton, 1995). However, when laurdan excitation GP spectra were calculated by labeling the membranes of 12 mammalian cell types, no evidence of phase domain coexistence was obtained (Parasassi et al., 1993a). Furthermore, laurdan GP studies on the influence of cholesterol on the dynamical properties of phospholipid phases showed that cholesterol has a "homogenizing" effect, which results in an increase in the dynamics of the gel phase and a decrease in that of the liquid-crystalline phase (Parasassi et al., 1994). The overall spectroscopic properties of cells were consistent with a picture of a homogeneously fluid-phase state, with restricted molecular motion compared to the pure phospholipid liquid-crystalline phase, and closely resembling the liquid-ordered phase described by Ipsen et al. (1987, 1989). In vesicles, the influence of cholesterol on the phospholipid phase state was found to depend on its absolute concentration. In particular, at peculiar cholesterol concentrations, abrupt modifications of the bulk lipid dynamical properties were observed (Parasassi et al., 1995). The fine modulation of structural and dynamical membrane properties at specific cholesterol concentrations was supported by recent findings by Virtanen et al. (1988, 1995) and by the Chong group (Tang and Chong, 1992; Chong et al., 1994; Chong, 1994) on presumed hexagonal lattice-type ordered molecular arrangements created at peculiar concentrations of a guest molecule in the phospholipid matrix, including cholesterol. In summary, from all of the above results the picture of the cell membrane dynamical properties appeared to be characterized by 1) the absence of gel-phase domains; 2) a homogeneous liquid-crystalline-like or liquid-ordered phase; 3) abrupt dynamical changes due to fine variations in cholesterol concentration. By extrapolating the results found in model membrane systems, it was hypothesized that in natural membranes the lipid dynamical properties could be finely tuned by small variations of the cholesterol concentration. In this liquid-crystalline-like ordered phase, it is noteworthy that laurdan spectroscopy could not reveal whether, in the presence of cholesterol, domains of different dynamical properties exist or not (Parasassi et al., 1994).

Microscopy can provide a unique tool for the study of membrane heterogeneity. However, the application of fluorescence spectroscopy methods to the microscope has been restricted, mainly because of the photolability of most of the membrane probes. Although there is a relatively extensive literature on membrane domains induced by protein segregation or similar induced effects (Rodgers and Glaser, 1991), the problem of the organization of the lipid components has not been extensively studied with the microscope. Recently, GP images of mouse fibroblast membranes labeled with laurdan were obtained with a two-photon fluorescence microscope (Yu et al., 1996) showing the existence of GP domains of different average GP values in the various cellular compartments. Possible artifacts due to the cell autofluorescence and to quenching by cellular components were excluded. Within each cellular membrane, the resultant GP domains were of very small size. A crucial observation was the broad distribution of GP values. One trivial explanation for the wide GP distribution was that of measurement noise. However, the possibility existed that the observed distribution reflected different local values of the GP. These observations stimulated more basic studies on model membrane systems for a characterization and understanding of the origin of the GP distribution. We reasoned that if we can perform simultaneous measurements of polarization and GP on each pixel, we can determine if there is a correlation between well-oriented membrane regions and GP values. From our previous knowledge on membrane packing and dynamics in phospholipid vesicles (Parasassi et al., 1990), we expected that more ordered regions (high polarization) should correspond to regions of relatively low water content (high GP). If this correlation can be demonstrated for well-identified membrane regions, then the GP distribution may correspond to a real membrane spatial heterogeneity.

In this work we present a study performed using lipid vesicles of different phase states and of coexisting phase states, with and without 30 mol% cholesterol. As a first approach to the study of the effect of cholesterol on phospholipid dynamics, the above cholesterol concentration was used, being representative of the average cell membrane cholesterol concentration (Levi et al., 1987). The lipid vesicles have been labeled with laurdan, and GP images have been acquired using our two-photon microscope. We also have acquired images of intact red blood cells, a renal tubular cell line, and renal apical brush border membranes and basolateral membranes with the purpose of comparing the results found in vesicles with the images of natural biological membranes.

MATERIALS AND METHODS

Lipid vesicle preparation

Multilamellar phospholipid vesicles were prepared by mixing the appropriate amounts of solutions in chloroform (spectroscopic grade) of phospholipids (dioleoyl-, dilauroyl-, dipalmitoylphosphatidylcholine, DOPC, DLPC, DPPC, respectively; Avanti Polar Lipids, Alabaster, AL) with or without cholesterol (Sigma Chemical Co., St. Louis, MO) and laurdan (Molecular Probes, Eugene, OR), then evaporating the solvent by nitrogen flow. The dried samples were resuspended in Dulbecco's phosphate-buffered saline (PBS) solution (pH 7.4) (Sigma Chemical Co.), heated above the transition temperature, and vortexed. The final total lipid and probe concentrations were 0.3 mM and 0.3 μM, respectively.

Fluorescence spectroscopy measurements

Fluorescence emission spectra of laurdan-labeled vesicles were obtained using a photon counting spectrofluorimeter (model GREG 200; ISS, Champaign, IL), equipped with a xenon arc lamp and photon-counting electronics (PX01; ISS) and thermostated at 20°C by a circulating water bath. The excitation generalized polarization (GP) spectra were calculated from the excitation spectra, acquired from 320 to 420 nm, using fixed emission

wavelengths of 440 nm or 490 nm, by

$$GP = (I_{440} - I_{490})/(I_{440} + I_{490}) \quad (1)$$

The two-photon polarization of laurdan was determined by using the same ISS spectrofluorimeter, except that the light source was a Ti-sapphire laser tuned at 770 nm, focused on the sample cuvette with a 5-cm focal length lens. The polarization determined for laurdan in glycerol at −20°C was 0.66, a value substantially larger than that obtained for one-photon excitation at 385 nm (0.44).

Red blood cell preparation

Approximately 5 ml of blood was drawn from a healthy laboratory volunteer in an EDTA-containing glass tube, and red blood cells (RBCs) were separated by centrifugation. The RBCs were then washed and resuspended in PBS.

Cell culture of opossum kidney cells

OK cells, a renal tubular epithelial cell line derived from the opossum kidney (Arar et al., 1995), were grown in a humidified 5% CO_2/95% air atmosphere in Dulbecco's modified Eagle's high-glucose medium (DMEM) containing 10% fetal calf serum, 100 IU/ml penicillin G, and 0.1 mg/ml streptomycin. For fluorescence microscopy measurements, cells were seeded on dishes containing microscope coverslips for 2–4 h. During this time the cells adhere to the coverslips, maintaining their round shape. The round shape was preferred for our experiments with polarized excitation.

Brush border and basolateral membrane preparation

Apical brush border (BBM) and basolateral (BLM) membranes from the rat renal cortex were simultaneously isolated by a differential centrifugation, magnesium precipitation, and discontinuous sucrose gradient method (Molitoris and Simon, 1985) as previously described (Levi et al., 1987, 1989). The BBM preparation was enriched at least 12-fold compared to the starting cortical homogenate, as assayed by the BBM-specific enzyme markers alkaline phosphatase, maltase, γ-glutamyl transferase, and leucine aminopeptidase specific activity. The BLM preparation was enriched at least 10-fold, compared to the starting cortical homogenate, as assayed by the BLM-specific enzyme marker Na,K-ATPase (Levi et al., 1987).

Two-photon microscopy measurements

Preparation of samples

Lipid vesicles. A drop of the lipid vesicle suspension was evaporated on a glass coverslip with a nitrogen stream. The coverslip was mounted on the microscope slide with a drop of distilled water.

OK cells. Laurdan labeling was performed directly on the culture dishes, adding 1 μl of a 2 mM probe solution in dimethyl sulfoxide (DMSO) per 1 ml of the growth medium and incubating for 30 min in the dark. Then the cells were gently washed with fresh medium and the coverslip was mounted on the microscope slide with fresh medium.

Red blood cells. About 20 μl of RBCs was diluted in 1 ml of PBS. Laurdan dissolved in DMSO was added to the suspension at a final concentration of 0.5 μM. At higher laurdan concentrations, the red cells were observed to lose their classical shape. After an incubation period of 30 min, the cells were washed once more and resuspended in 1 ml of buffer. About 100 μl of the solution was transferred to a hanging drop slide and sealed with a coverslip. The coverslip was covered with a hydrophobic silane layer to help maintain the round cell shape.

BBM and BLM membranes. Purified membranes were diluted to a concentration of 0.1 mg protein/ml. Laurdan labeling was performed by adding 1 μl of the 2 mM probe solution in DMSO per 1 ml of the membrane sample. The sample was vortexed for 30 s at room temperature. Then a drop of the membrane preparation was evaporated on a coverslip with a nitrogen stream. The coverslip with the dried membrane was mounted on the microscope slide with a drop of distilled water.

Experimental apparatus for two-photon excitation microscopy measurements

Two-photon excitation is a nonlinear process in which a fluorophore absorbs two photons simultaneously. Each photon provides half the energy required for excitation. The high photon densities required for two-photon absorption are achieved by focusing a high peak power laser light source on a diffraction-limited spot through a high numerical aperture objective. Hence, in the areas above and below the focal plane, two-photon absorption does not occur, because of insufficient photon flux. In this manner the two-photon method provides a depth discrimination or sectioning effect similar to that of confocal microscopy without using emission pinholes. For example, when 770-nm excitation (which results in a two-photon absorption equivalent to 385-nm excitation) is used with a 1.25 NA objective, over 80% of the total fluorescence intensity is confined to within 1 μm of the focal plane (So et al., 1995, 1996). Another advantage of the two-photon excitation is the significant reduction of photobleaching and photodamaging in areas above and below the focal plane.

The data acquisition and image analysis methods for GP microscopy measurements as described by Yu et al. (1996) were followed. A titanium-sapphire laser (Mira 900; Coherent, Palo Alto, CA) pumped by an argon ion laser (Innova 310; Coherent) was used as the excitation light source because of its stability. The wavelength of the laser was tuned at 770 nm, where it has maximum power. The laser light was guided by a galvanometer-driven x-y scanner (Cambridge Technology, Watertown, MA) to achieve beam scanning in both the x and y directions. The scanning rate was controlled by the input signal from a frequency synthesizer (Hewlett-Packard, Santa Clara, CA), and a frame rate of 9 s was used to acquire the three images (256 × 256 pixels) for the GP calculation. The laser power was attenuated to 20 mW before the light entered the microscope. The sample receives about one-tenth of the incident power. A quarter-wave plate (CVI Laser Corporation, Albuquerque, NM) was placed after the polarizer to change the polarization of the laser light from linear to circular for polarization-independent excitation. To change the laser polarization, a polarizer was placed right after the quarter-wave plate in the excitation path. Two optical bandpass filters (Ealing Electro-Optics, New Englander Industrial Park, Holliston, MA) were used to collect fluorescence in the blue and red regions of the laurdan emission spectrum. A miniature photomultiplier (R5600-P; Hamamatsu, Bridgewater, NJ) amplified through a AD6 discriminator (Pacific, Concord, CA) was used for light detection in the photon counting mode. The counts were acquired by a home-built card.

RESULTS

Spectroscopy

Laurdan fluorescence excitation and emission spectra, GP values, and GP spectra in phospholipid vesicles in the gel and in the liquid-crystalline phases and the effect of cholesterol have been extensively reported in previous papers (Parasassi et al., 1990, 1994; Parasassi and Gratton, 1995). For clarity, here we recall some of the emission spectral features of this probe and of its excitation GP spectra. We also present new spectroscopic data on the equimolar mixture composed of DOPC and DPPC.

In Fig. 1 *A*, laurdan emission spectra at 20°C of vesicles in the liquid-crystalline phase (DOPC and DLPC vesicles), in the gel phase (DPPC vesicles), and in the equimolar mixture of two coexisting phases (DOPC/DPPC and DLPC/DPPC vesicles) are reported. Because of dipolar relaxation, in liquid-crystalline vesicles a red shift of the emission can be observed, which is more pronounced in DOPC vesicles. The laurdan emission in gel-phase DPPC vesicles is narrow and blue. In vesicles composed of mixed phases, the emission spectrum is broad, because of both blue and red emitting laurdan molecules. The corresponding excitation GP spectra are reported in Fig. 1 *B*. Excitation GP spectra show laurdan GP values obtained at the different excitation wavelengths, from 320 nm to 420 nm. Characteristic features of the laurdan excitation GP spectra can be summarized as follows: 1) In the gel phase (DPPC vesicles), no appreciable wavelength dependence of the GP value can be observed. 2) In the liquid-crystalline phase (DOPC and DLPC vesicles), the GP value decreases with increasing excitation wavelength. This behavior has been explained as being due to an increasing excitation of the relaxed laurdan molecules populating the red part of the excitation band as the excitation wavelength is increased. 3) In the presence of coexisting phases (equimolar mixtures of DOPC/DPPC and of DLPC/DPPC), the red part of the excitation spectrum corresponds to laurdan molecules surrounded by phospholipids in the gel phase, so that as the excitation wavelength is increased, more unrelaxed (blue emitting) laurdan molecules are excited, resulting in an excitation GP spectrum with a positive slope. This opposite behavior of laurdan excitation GP spectra, with a positive slope in the presence of mixed phases and a negative slope in the liquid-crystalline phase, has been used to discriminate between membranes composed of two coexisting or one-phase phospholipids (Parasassi et al., 1993a,b; Parasassi and Gratton, 1995). In Fig. 2 *A* we report the laurdan emission spectra obtained in the same samples with the addition of 30 mol% cholesterol. The presence of 30 mol% cholesterol noticeably reduces the dipolar relaxation effect, resulting in a blue shift of the emission spectra observed in all samples. The excitation GP spectra of the samples with 30 mol% cholesterol are reported in Fig. 2 *B*. Compared with the same samples without cholesterol, we can observe a general increase in the absolute GP values. Furthermore, a modification of their wavelength dependence can be observed, the excitation GP spectra being relatively flat, similar to the excitation GP spectra observed in gel phase without cholesterol. In the phospho-

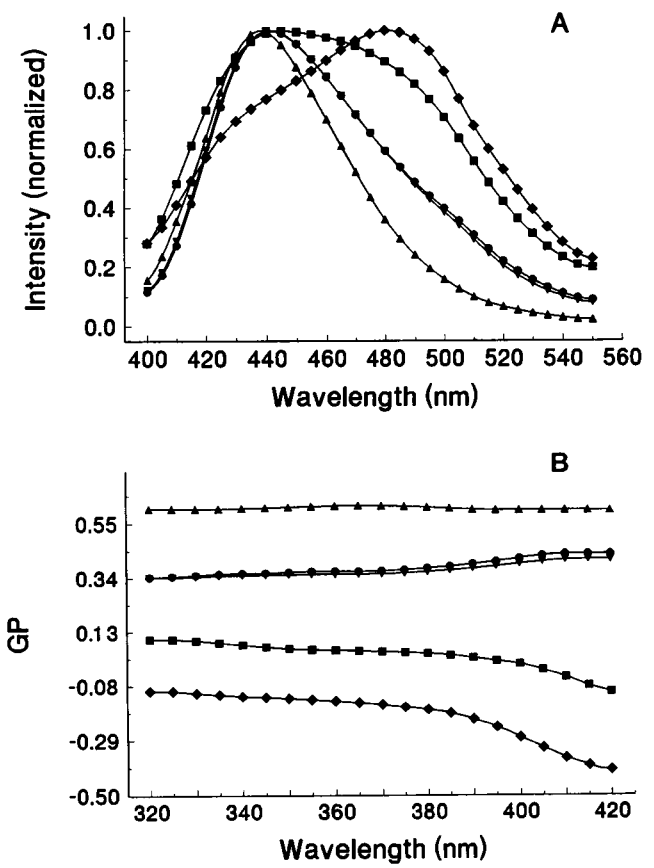

FIGURE 1 Normalized laurdan fluorescence emission spectra (*A*) and excitation GP spectra (*B*) in multilamellar phospholipid vesicles composed of DOPC (♦), DLPC (■), and DPPC (▲) and of equimolar mixtures of DOPC and DPPC (▼) and of DLPC and DPPC (●) at 20°C.

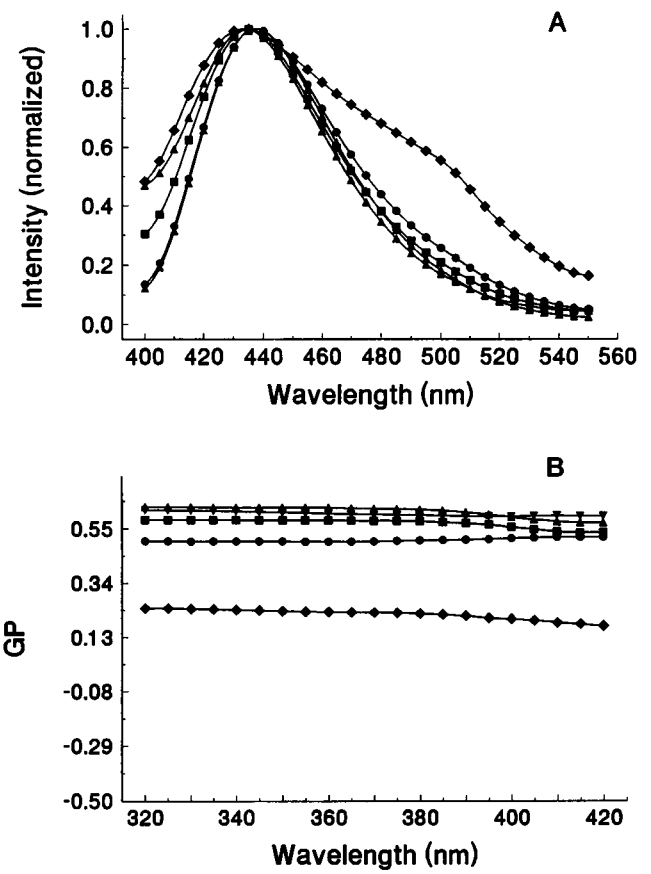

FIGURE 2 Normalized laurdan fluorescence emission spectra (*A*) and excitation GP spectra (*B*) in multilamellar phospholipid vesicles composed of 30 mol% cholesterol and DOPC (♦), DLPC (●), DPPC ([trif) and of equimolar mixtures of DOPC and DPPC (▼) and of DLPC and DPPC (■) at 20°C.

lipid mixtures and in the presence of cholesterol, the typical spectral features of two coexisting phases as opposed to the liquid-crystalline phase cannot be observed. These results have previously been discussed in terms of an opposite effect of cholesterol on the dynamic properties of the two pure phases, with the consequence of a homogenizing effect on the membranes that are composed of coexisting phases (Parasassi and Gratton, 1995). In the presence of cholesterol, a relatively small wavelength dependence of the GP value can be observed in the samples composed of pure phospholipids, DOPC, DLPC, and DPPC, only at high excitation wavelengths, above 390 nm, with a slightly negative slope as the excitation wavelength increases.

Microscopy

Vesicles without cholesterol

Images of vesicles composed of the above phospholipids and labeled with laurdan have been obtained with the two-photon excitation fluorescence microscope, using polarized laser excitation. Although we present images of selected fields of view, the entire slide presents a remarkable homogeneity. Different regions have almost identical GP histograms, although the shape of the vesicles may vary from region to region. Under white light, vesicles appear approximately spherical. Because of the sectioning effect of the two-photon microscope, a section ~600 nm thick is imaged for each scan. In Fig. 3 the section images of the DOPC vesicles at room temperature (~20°C) are shown. The different colors represent different laurdan GP values, following the scale reported in the figure. The GP values are relatively low, mainly below 0, as expected in vesicles in the liquid-crystalline phase. In all images presented, the average GP value is in excellent agreement with that measured in cuvette studies. A novel result from the microscope images is that the distribution of the GP values is broad, indicating a relevant heterogeneity of the vesicles (Fig. 4 *A*). Polarized excitation allows a better understanding of the heterogeneity of the vesicles. Polarized excitation (~10° with respect to the horizontal) apparently photoselects areas (pixels) of higher GP value. The photoselection due to polarized light obtained by two-photon excitation is more pronounced than the photoselection obtained by one-photon excitation, because of the larger value of the time 0 polarization of laurdan (0.66 at 770 nm versus 0.44 at 385 nm). By selectively plotting only the pixels below and above the average value of the GP distribution (GP < -0.2, Fig. 3 *B*; GP > -0.2, Fig. 3 *C*), different, nonoverlapping areas are drawn. Because of the photoselection operated by the polarized excitation, mainly the pixels with higher GP values are plotted along the axis parallel to the excitation axis (Fig. 3 *C*). The heterogeneity of the liquid-crystalline phase is even more evident in the images of the DLPC vesicles (Fig. 5). Also for these vesicles, the broad GP histogram (Fig. 4 *B*) corresponds to disjoined spatial regions (Fig. 5 *A*). Excitation polarization photoselection can clearly be seen by plotting of the pixels with GP < 0 or GP > 0 (Fig. 5, *B* and *C*). The images obtained from DPPC vesicles are shown in Fig. 6. In this gel-phase sample, the GP values are high and relatively homogeneous (see the relatively narrow histogram in Fig. 4 *C*). The excitation polarization photoselection is barely visible. In Fig. 6, *B* and *C*, the images of the areas of the DPPC vesicles with GP < 0.45 and GP > 0.45, respectively, are reported. The selected regions do not cor-

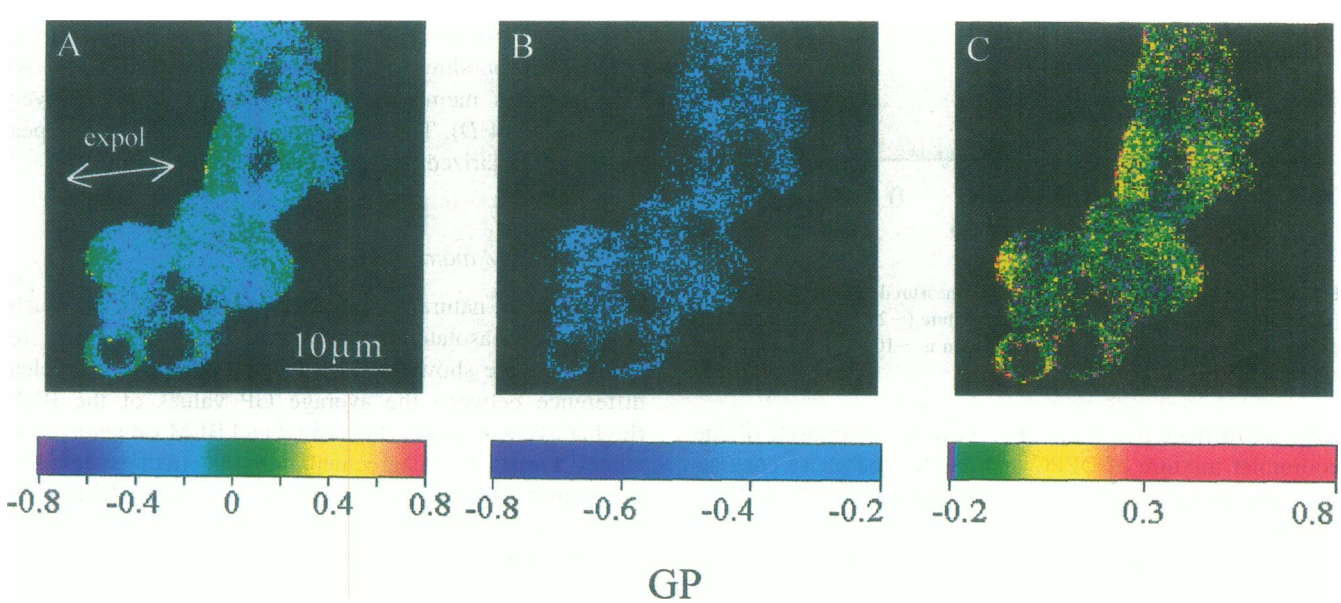

FIGURE 3 GP images of DOPC vesicles labeled with laurdan at room temperature (~20°C). The colors indicate different GP values following the reported scale. The image scale bar is reported in *A*, together with the direction of the excitation polarization. In *B* and *C* only selected GP values are drawn, using the colors indicated in the corresponding scales. Polarized excitation light has been used; the direction of polarization is ~10° with respect to the horizontal.

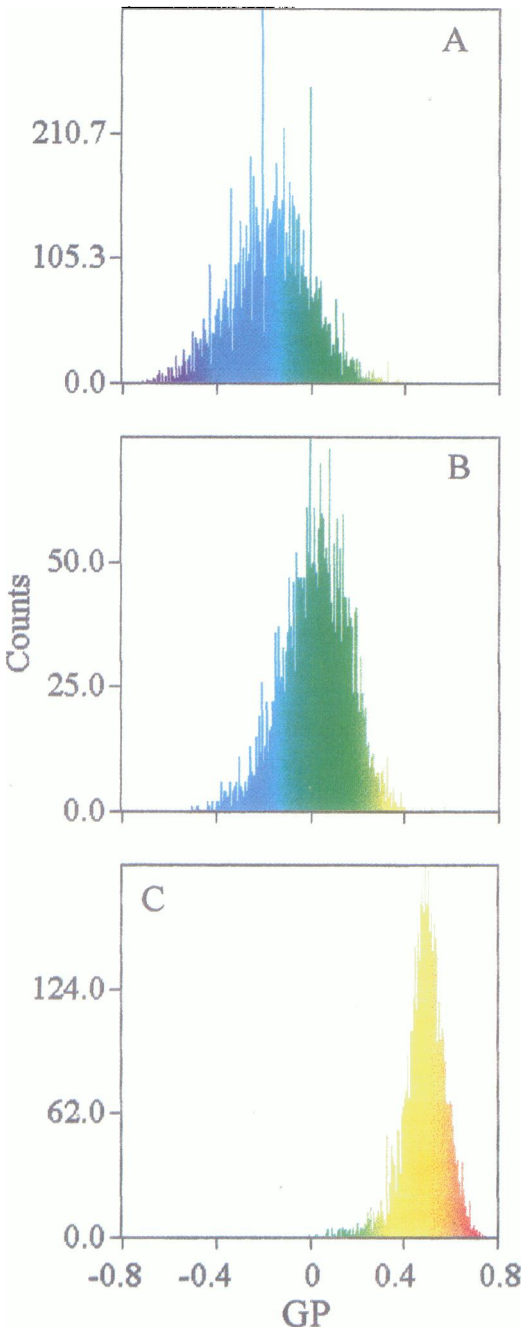

FIGURE 4 Histograms of the GP values measured in DOPC (*A*), DLPC (*B*), and DPPC (*C*) vesicles at room temperature (~20°C), using polarized excitation light. The direction of polarization is ~10° with respect to the horizontal.

respond to disjoined areas. For vesicles composed of the equimolar mixture of DPPC and DOPC, the phase coexistence is impressively clear in the GP image (Fig. 7), both for the spread of the GP histogram (Fig. 8 *A*) and for the photoselection operated by the polarized excitation (Fig. 7).

Vesicles with 30 mol% cholesterol

The presence of cholesterol induces remarkable modifications in the images presented above. The images of the DPPC sample with cholesterol (Fig. 9) appear almost completely "polarized," with a very low intensity in the vertical plane, perpendicular to the horizontal excitation polarization. The histogram of the GP distribution (Fig. 8 *B*) is relatively narrow but shifted to higher GP values, and shows a tail of low intensity with lower GP values. The pixels with low GP value are uniformly distributed in the membrane (Fig. 9 *B*), rather than located in disjoined large regions. In the vesicles composed of the equimolar mixture of DOPC and DPPC, the presence of 30 mol% cholesterol produces a narrowing of the GP histogram (Fig. 8 *C*), and the images appear strongly polarized (Fig. 10). When low and high GP values (lower or higher than 0.3) are plotted, the excitation photoselection is clearly observable (Fig. 10, *B* and *C*). When the excitation is unpolarized, a more complex pattern appears (Fig. 11). The characteristic annular shape of the vesicles is due to the particular section of this image that is close to the bottom of the vesicles.

RBC and OK cells

The images of intact RBCs are shown in Fig. 12 *A*. The section is through the center of the cell. The GP histogram is relatively wide (Fig. 12 *D*). Sectioning of the histogram in low GP and high GP produces the images of Fig. 12, *B* and *C*. One remarkable feature of Fig. 12, *B* and *C*, is that the regions of low and high GP are not disjoined, but the high GP image is well polarized, whereas the low GP image has pixels uniformly distributed around the cell membrane. OK cells have a large amount of fluorescence from internal membranes (Fig. 13 *A*). When only GP values greater than 0.3 are plotted, the plasma membrane is isolated with higher intensity (pixel density) parallel to the excitation polarization (Fig. 13 *C*). To isolate the external membrane, we have masked the pixels in the cell interior and left only those pixels corresponding to the plasma membrane (Fig. 14 *A*). Only for this membrane is the GP histogram relatively broad (Fig. 14 *D*). The images of low and high GP appear to be well polarized and disjoined (Fig. 14, *B* and *C*).

BBM and BLM membranes

GP images of natural membranes, purified rat renal brush-border, and basolateral membranes (BBM and BLM, respectively) are shown in Fig. 15. We can observe a clear difference between the average GP values of the BBM (higher average values; Fig. 15 *C*) and BLM (lower average values; Fig. 15 *F*), in agreement with the effect expected for the higher cholesterol concentration of the BBM membranes (Levi et al., 1987, 1989, 1990). Excitation polarization photoselection cannot be observed, probably because of the complex shape of these membrane preparations. Instead, in the GP images, a complex texture of different, separate, coexisting GP values can be observed (Fig. 15, *A* and *D*). Images obtained at selected GP values show well-resolved microscopic structures. In addition, the borders of the mem-

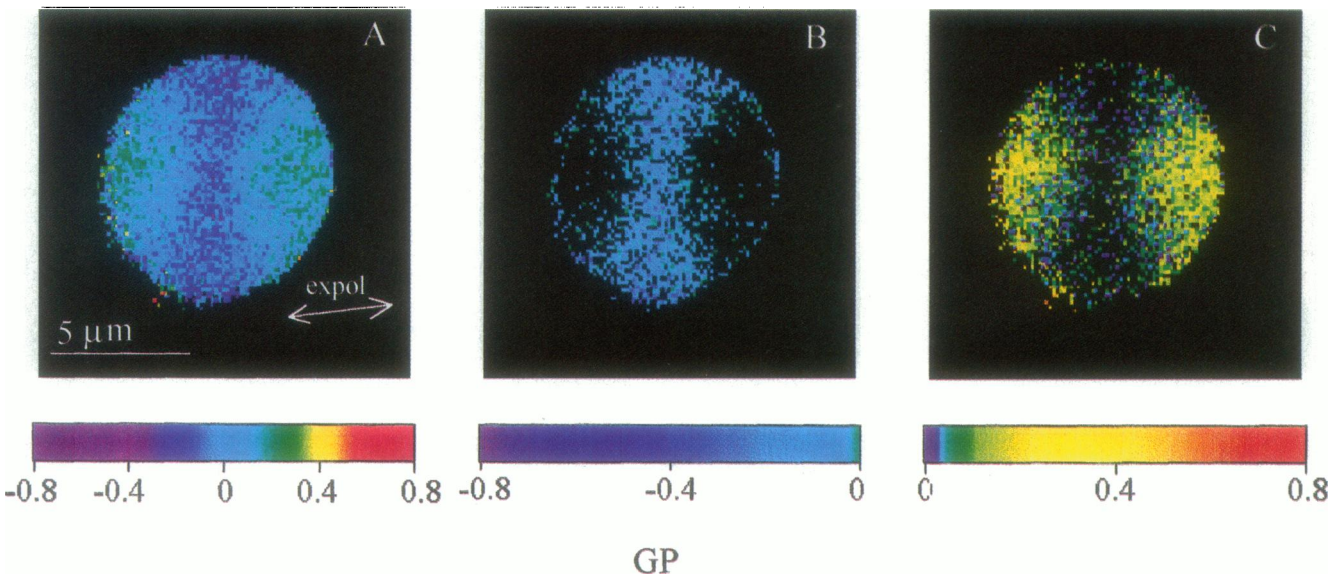

FIGURE 5 GP images of DLPC vesicles labeled with laurdan at room temperature (~20°C). The colors indicate different GP values following the reported scale. The image scale bar is reported in *A*, together with the direction of the excitation polarization. In *B* and *C* only selected GP values are drawn, using the colors indicated in the corresponding scales. Polarized excitation light has been used; the direction of polarization is ~10° with respect to the horizontal.

branes can be isolated by plotting only relatively low GP values (Fig. 15, *B* and *E*).

DISCUSSION

The effect of photoselection and the interpretation of the GP images

As the first point in our discussion, we want to emphasize the importance of the GP measurement using polarized excitation light. Indeed, GP images of mouse fibroblast membranes have previously been reported, showing the coexistence of several areas of different average GP values (Yu et al., 1996). Furthermore, identifiable membrane structures, such as the plasma membrane and the nuclear membrane, could be highlighted by plotting selected GP windows. For example, the plasma membrane showed larger GP values than the nuclear membrane. However, neither the meaning of the broad GP distribution nor the contribution of measurement noise to the degree of GP distribution was previously discussed. For a better interpretation of the GP

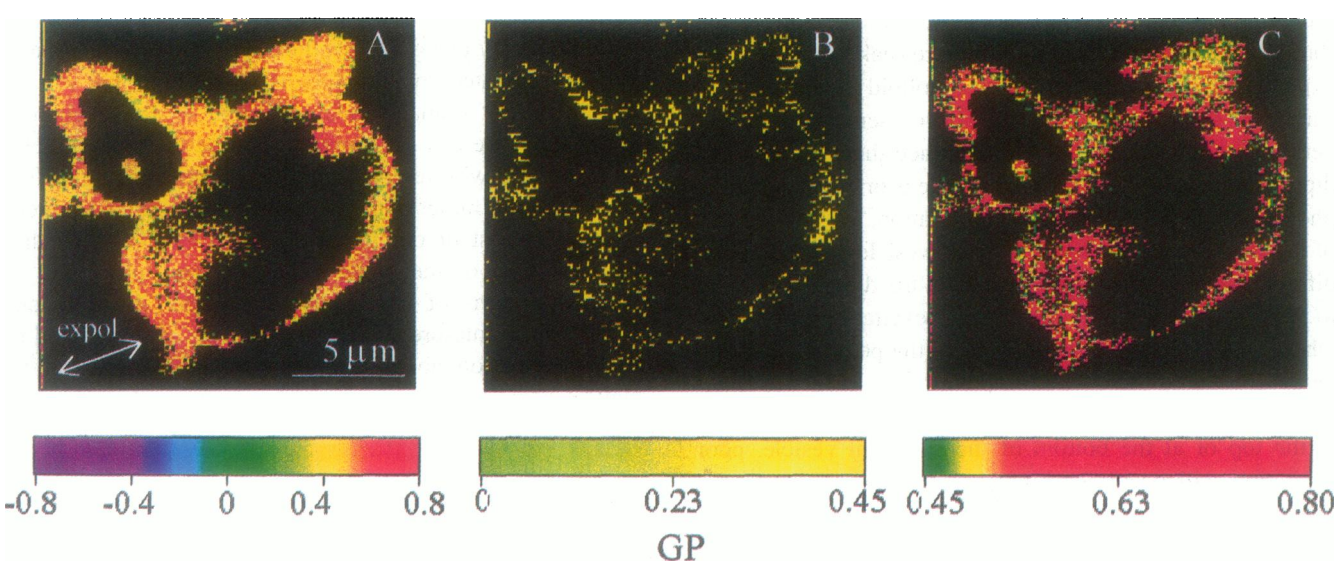

FIGURE 6 GP images of DPPC vesicles labeled with laurdan at room temperature (~20°C). The colors indicate different GP values following the reported scale. The image scale bar is reported in *A*, together with the direction of the excitation polarization. In *B* and *C* only selected GP values are drawn, using the colors indicated in the corresponding scales. Polarized excitation light has been used; the direction of polarization is ~20° with respect to the horizontal.

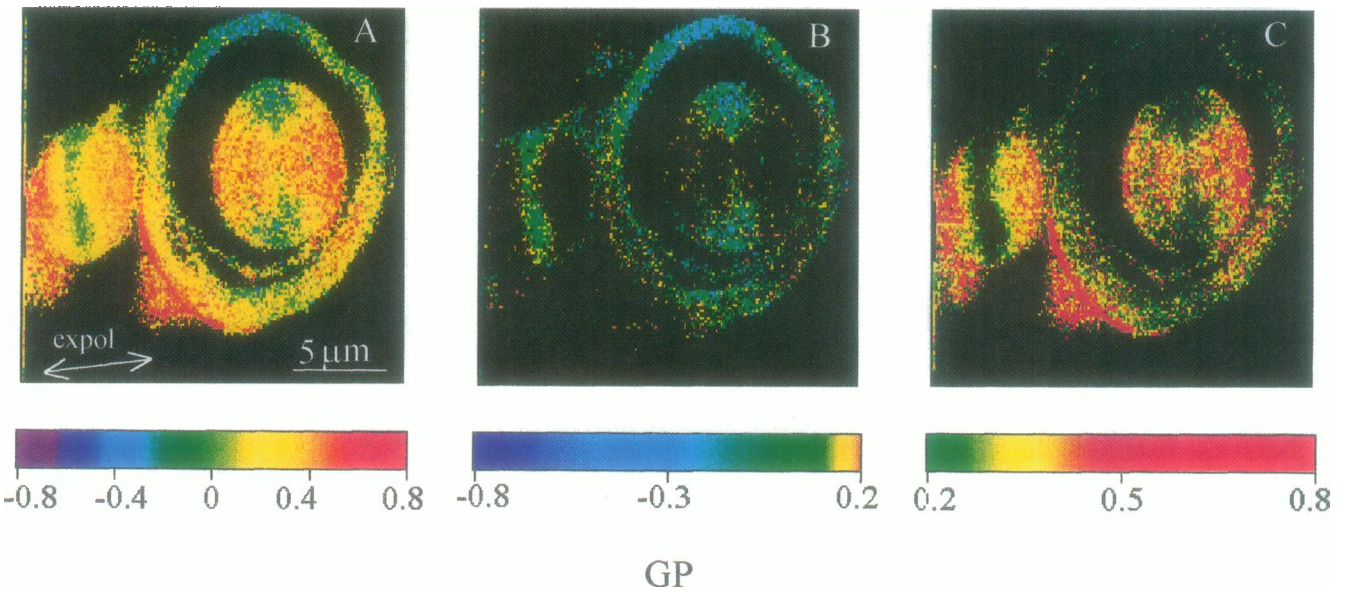

FIGURE 7 GP images of vesicles composed of the equimolar mixture of DOPC and DPPC labeled with laurdan at room temperature (~20°C). The colors indicate different GP values following the reported scale. The image scale bar is reported in *A*, together with the direction of the excitation polarization. In *B* and *C* only selected GP values are drawn, using the colors indicated in the corresponding scales. Polarized excitation light has been used; the direction of polarization is ~10° with respect to the horizontal.

distribution, we performed a series of experiments on lipid vesicles using polarized excitation, the results of which we present here. The interpretation we propose for the observed GP patterns is based on a model that takes into account the sectioning effect of the two-photon microscope and the supposedly relatively well-organized structure of multilamellar vesicles, which allowed us to correlate regions of different GP with regions of different orientation of the laurdan molecules (see Fig. 16 for a diagram of various possibilities). We assume that our microscope images correspond to a section through the onionlike structure of the multilamellar vesicle. Sections at the center or at the top (bottom) of the multilamellar structure make it possible to explore regions of different phospholipid orientation, as shown schematically in Fig. 16. From a series of independent measurements, we have determined that the transition dipole moment of the laurdan molecule is oriented along the phospholipid chain (Parasassi and Gratton, 1995). Because of the well-organized structure of the vesicle, as we explore different sections of a large vesicle, in the direction parallel to the excitation polarization strong excitation can occur, whereas poor excitation will occur in the polar regions and perpendicular to the excitation polarization (Fig. 16, Excitation photoselection panel). Furthermore, in the z section, at the top or at the bottom of the spherical vesicle, poor excitation will occur for bilayers with phospholipids and laurdan molecules oriented along the z axis. Therefore, excitation in the polar regions and along the z axis may only occur in a disordered phase, with laurdan molecules oriented with a component along the equatorial direction. Note that the proposed identification of photoselection effects in our images is based on the presumed knowledge of the morphology of the membrane. A similar reasoning about photoselection also applies to sections of discoid shapes or planar bilayers. For structures smaller than the microscope resolution, photoselection by polarized excitation still operates, but an average GP value will be measured, weighted by the distribution of orientations of the particular structure (Fig. 16, GP spatial distribution panel).

Our crucial experimental observation is that polarized light, which photoselects well-oriented laurdan molecules, also selects laurdan molecules associated with high GP values. This is in itself a remarkable finding, because it allows us to gain confidence about the meaning of the GP distribution. By using polarized excitation, when the image contains separated domains (pixels) of different GP values, the higher GP domains being parallel to the excitation polarization, we can determine that these domains (pixels) are associated with regions of the membrane having different GP values, rather than being the effect of measurement noise. For most of our images we can clearly show that different parts of the broad GP histogram correspond to different regions of the image. To further illustrate our model for the interpretation of the patterns observed and to infer information about the size of the domains, let us analyze some limiting theoretical situations (Fig. 16, GP spatial distribution panel).

The laurdan molecule in a homogeneous environment

In this case the GP distribution is narrow. If the membrane is ordered (such as DPPC vesicles at 20°C), polarized excitation in the vesicle structure may result in equatorial

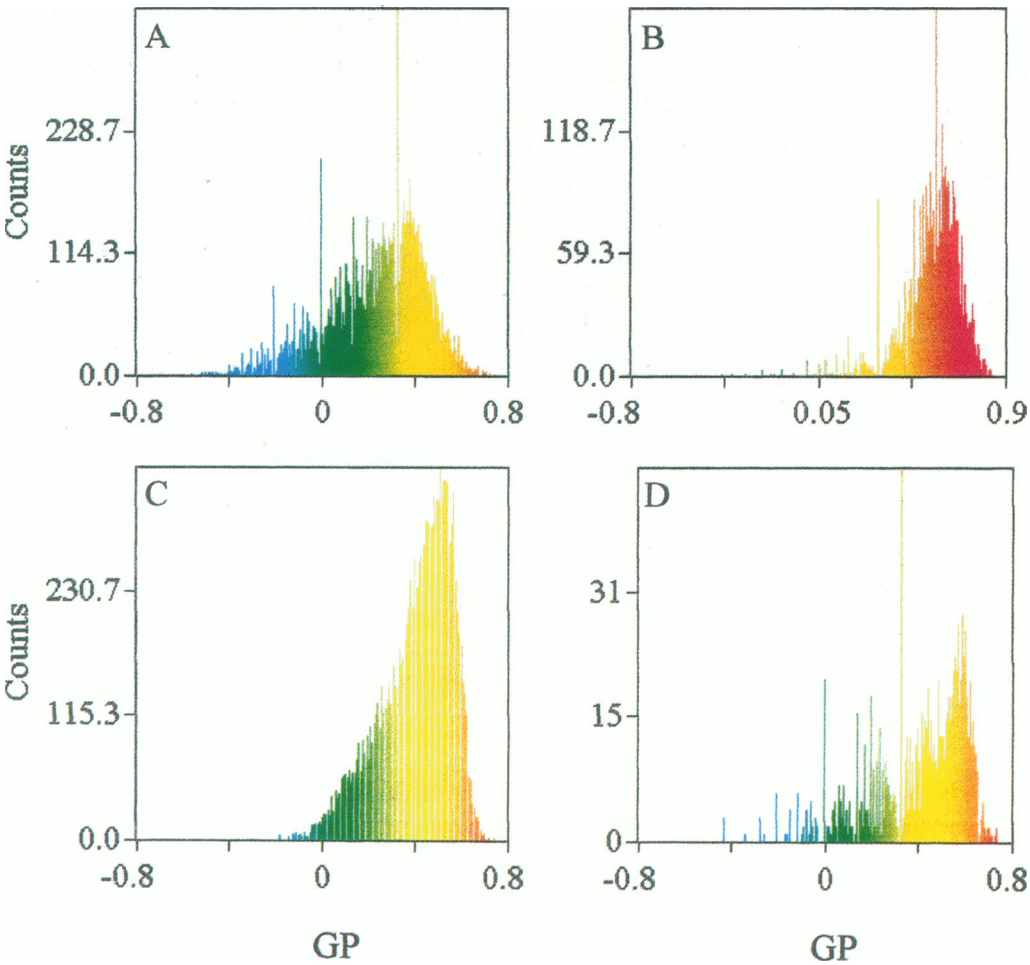

FIGURE 8 Histograms of the GP values measured in vesicles composed of the equimolar DOPC and DPPC mixture (*A*), of DPPC with 30 mol% cholesterol (*B*), and of the equimolar DOPC and DPPC mixture with 30 mol% cholesterol (*C*). The experiments relative to *A*, *B*, and *C* have been performed with polarized excitation. (*D*) Histogram of the same sample as in *C*, but excited by depolarized light. Measurements were made at at room temperature (~20°C).

regions of substantial higher total fluorescence emission. However, the GP image, which results only from spectral differences and not by different orientations, should be relatively uniform both in the equatorial and in the polar regions of the vesicle. Of course, it may happen that in the polar regions there is not enough intensity to measure the GP. Our image-processing software only calculates the GP in those pixels with adequate intensity. If the laurdan molecule can have every possible orientation in every location in the vesicle, the total fluorescence intensity (as well as the GP) should be spatially homogeneous.

The environment of the laurdan molecule is heterogeneous because of the presence of domains of different GP values

In this case the GP distribution is broad or bimodal. 1) If the domains are smaller than the microscope resolution, in every pixel there are both kinds of domains. Because "rigid" domains are well oriented, they are preferentially excited in the direction of the light polarization (equatorial), and laurdan molecules with high GP are preferentially observed in this direction. In the perpendicular direction (polar) only the "more fluid" domains can be excited. In this case, the GP image appears to be "polarized," with an almost perfect separation between the equatorial region (selection of the ordered regions) and the polar regions (selection of the fluid regions); this is the characteristic signature of the coexistence of rigid and fluid domains smaller than the microscope resolution. Note that this reasoning holds only in relatively large, well-organized sections of the lamellar structure. 2) If the domains are much larger than the microscope resolution, then clearly separated regions with different GP should be observed. 3) If the domains have a size comparable to the pixel size or if there is a broad distribution of domain sizes, then polarized excitation selects regions of high GP (rigid domains), so that the image of the pixels with high GP is essentially in the equatorial plane. However, because the domains are relatively large, there may also be excitation of relatively low GP domains (fluid domains) in both equato-

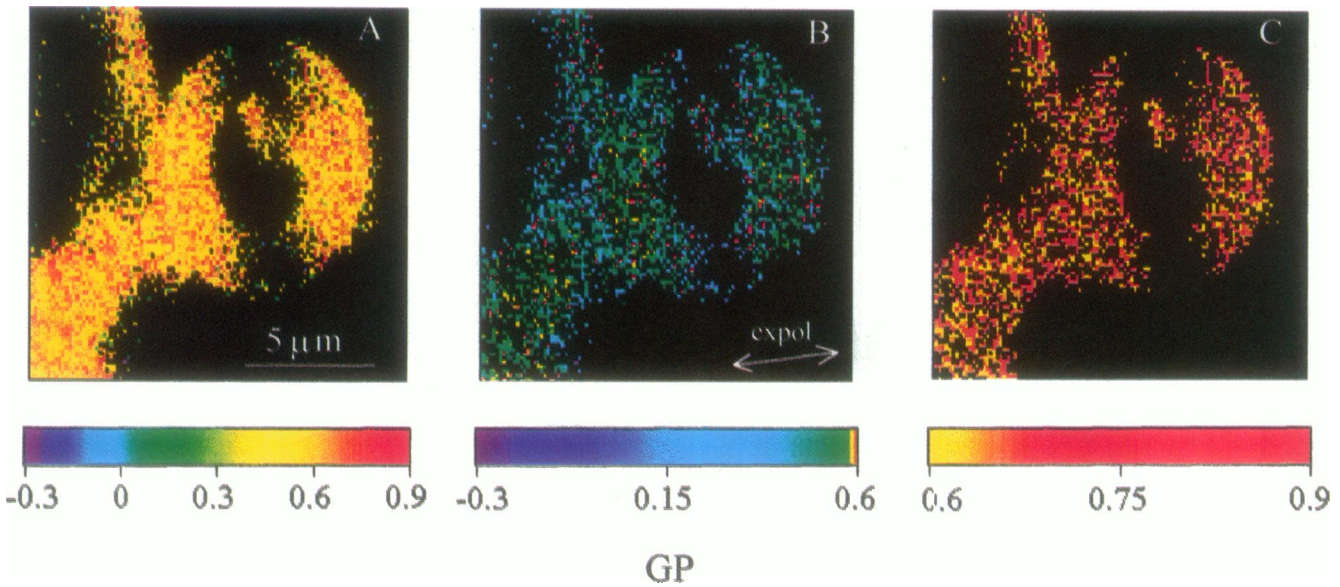

FIGURE 9 GP images of vesicles composed of DPPC and 30 mol% cholesterol labeled with laurdan at room temperature (~20°C). The colors indicate different GP values following the reported scale. The image scale bar is reported in *A*, together with the direction of the excitation polarization. In *B* and *C* only selected GP values are drawn, using the colors indicated in the corresponding scales. Polarized excitation light has been used; the direction of polarization is ~10° with respect to the horizontal.

rial and polar regions, because these domains are poorly polarized. As a consequence, the image of the low GP values is uniformly distributed in the equatorial and polar regions. This is the characteristic signature of coexisting domains with sizes comparable to the microscope resolution. Of course, to observe domains of this size, the contribution from the different layers of the multilamellar vesicles should be separated, i.e., only in unilamellar vesicles or in cell membranes made of a well-identified single bilayer can this effect be observed. Furthermore, these large microdomains should last for times longer than the total time for the GP image acquisition (~27 s).

Possible origin of the broad GP distribution of the liquid-crystalline phase

We have a series of novel observations with regard to previous models of dynamical properties of phospholipid

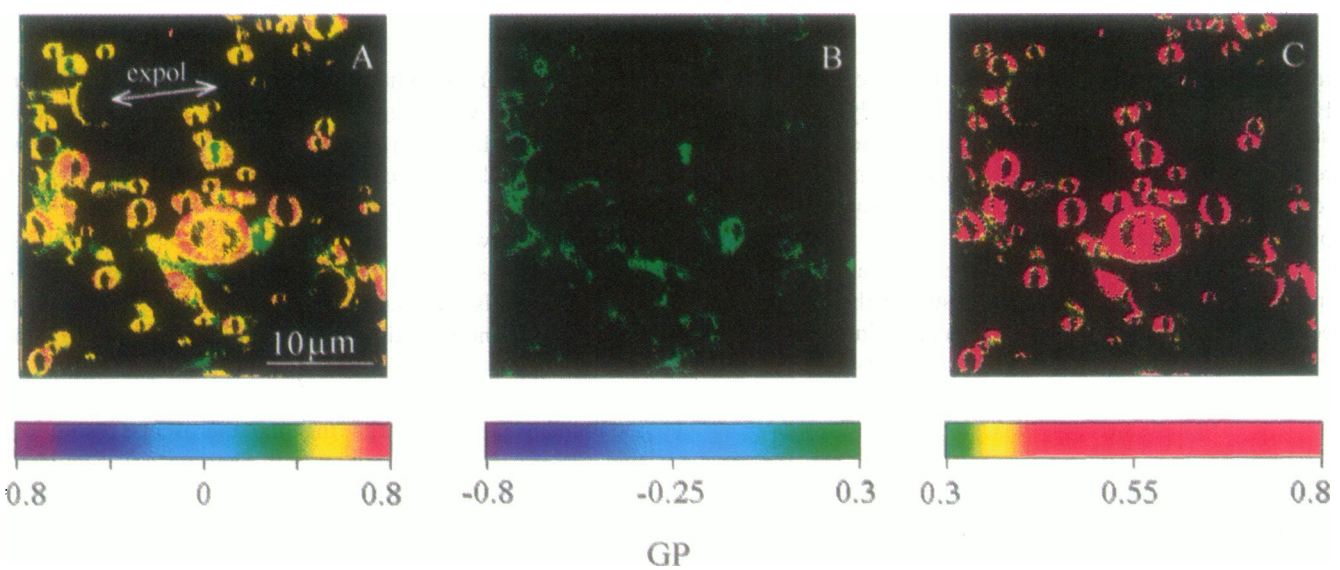

FIGURE 10 GP images of vesicles composed of the equimolar DOPC and DPPC mixture, with 30 mol% cholesterol, labeled with laurdan at room temperature (~20°C). The colors indicate different GP values following the reported scale. The image scale bar is reported in *A*, together with the direction of the excitation polarization. In *B* and *C* only selected GP values are drawn, using the colors indicated in the corresponding scales. Polarized excitation light has been used; the direction of polarization is ~10° with respect to the horizontal.

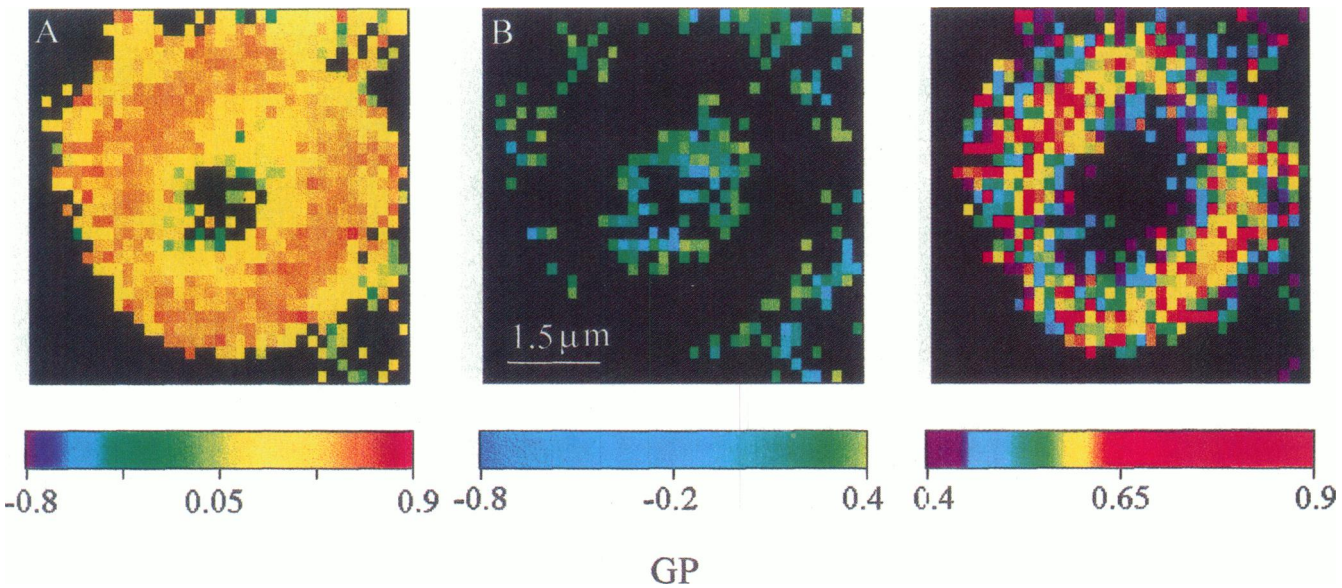

FIGURE 11 GP images obtained with the same sample as in Fig. 10, but with excitation by depolarized light.

bilayers and of the effect of cholesterol. In vesicles composed of a single phospholipid (i.e., of a single phase), an unexpected finding of our microscopic observations concerns the existence of a large dynamical heterogeneity, particularly in the liquid-crystalline phase. In both DOPC and DLPC vesicles, the GP distributions are surprisingly broad (Fig. 4, *A* and *B*). We can observe a strong photoselection of higher GP values in the equatorial regions and low GP values in the polar regions of our multilamellar vesicles. In the GP images of DLPC vesicles, the separation between equatorial and polar regions is particularly strong (Fig. 5). According to our interpretation model, the size of the GP domains must be smaller than the microscope resolution, which is ~200 nm radially and 600 nm axially. The small size of the microdomains can arise either because along a single layer of the multilamellar vesicle the domains are small or because the layers are so close that the contribution from individual layers cannot be resolved. For a vesicle in the liquid-crystalline phase we were expecting a relatively homogeneous fluid environment of the laurdan molecule. However, our experiments show that the liquid-crystalline phase is made of a distribution of small domains, which are stable enough to be observed as separate entities during the fluorescence lifetime of laurdan, which is ~4 ns in the liquid-crystalline phase. We propose that the intrinsic heterogeneity of the liquid-crystalline phase is due to a distribution of different sites in which the laurdan molecule can reside. These sites are characterized by a different number of water molecules, and we have already demonstrated that the GP value is sensitive to the membrane water content (Parasassi and Gratton, 1995). On the basis of NMR studies (Borle and Seelig, 1983) and molecular dynamics calculations (Chiu et al., 1995), we estimate that the average number of water molecules at the location of the laurdan fluorescent moiety is not more than two or three. Because of the Poisson distribution of these few water molecules, there is a distribution of laurdan environments with no, one, two, three, etc. molecules of water. For example, for an average of two molecules of water per cavity around the laurdan fluorescent moiety, the Poisson distribution of water molecules at the different sites is $0 \rightarrow 0.135$, $1 \rightarrow 0.270$, $2 \rightarrow 0.270$, $3 \rightarrow 0.203$, $4 \rightarrow 0.090$, $5 \rightarrow 0.031$, and more than $5 \rightarrow 0.020$, The larger the number of water molecules, the lower is the GP, and the larger is the cavity around the laurdan molecule. Because of photoselection operated by polarized excitation, in the polar regions, perpendicular to the excitation photoselection, we can excite laurdan molecule in large cavities, whereas in the equatorial regions, parallel to the excitation photoselection, we preferentially excite laurdan molecules in small cavities. This model explains why low GP values are correlated with poorly oriented laurdan molecules. Instead, in DPPC vesicles, which contain virtually no water at 20°C, the GP distribution is narrow (Fig. 4 *C*), and the intensity arises almost completely from the equatorial regions (data not shown). The GP image is relatively uniform (Fig. 6), in accord with expectations for a homogeneous sample. In these pure gel-phase vesicles, the GP value was previously shown to be constant with temperature and only dependent on the bilayer phase state, but not on its composition (Parasassi and Gratton, 1995). Within the liquid-crystalline phase a temperature increase is known to cause a decrease in the laurdan GP to an asymptotic value (Parasassi et al., 1990). On the basis of our new findings of the GP distributions in the liquid-crystalline phase, we propose that this effect is caused by a gradual increase of sites with more water as the temperature increases. To support this point of view, we compare the GP images of the DOPC and DLPC vesicles. Both vesicles are in the liquid-crystalline phase at 20°C, but DLPC is closer to the transition temperature than DOPC. In the image of the

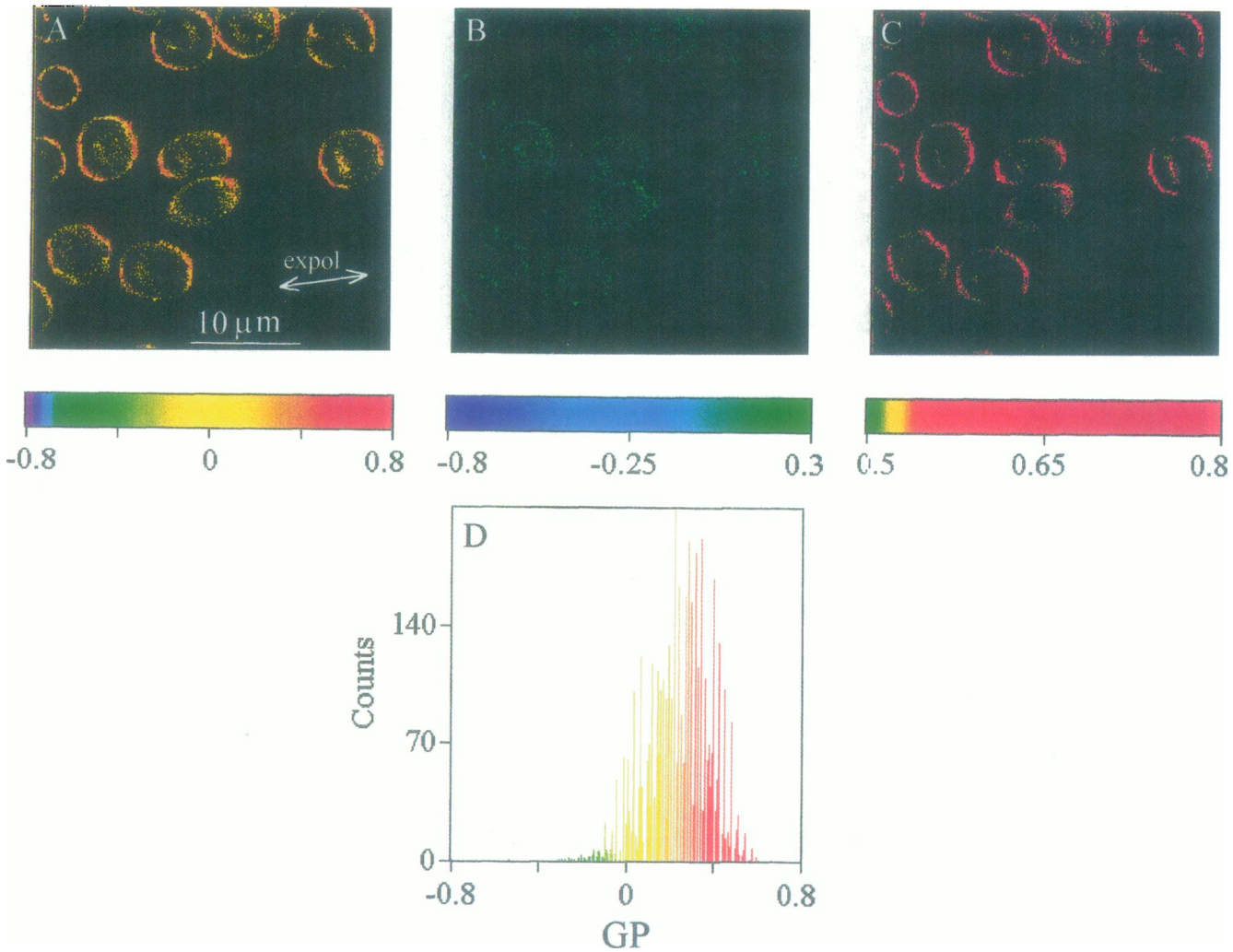

FIGURE 12 (*A*) GP images of red blood cells labeled with laurdan obtained at room temperature (~20°C). The colors indicate different GP values following the reported scale. In *B* and *C* the low and high GP values are drawn, respectively, following the reported scales. (*D*) Distribution of the GP values. The image scale bar is reported in *A*, together with the direction of the excitation polarization.

DLPC vesicles, regions of different GP are more disjoined. We note that, in cuvette studies, neither the flat excitation GP spectrum of the gel phase nor the wavelength dependence of the excitation GP spectrum in the liquid-crystalline phase could detect the heterogeneity shown by the microscopic observations.

In equimolar mixtures of DOPC/DPPC, the gel and liquid-crystalline domains are small

The microscopy images of the vesicles composed of an equimolar mixture of the two phospholipid phases (DOPC and DPPC) show the occurrence of regions of different GP values (Fig. 7). The GP histogram is quite broad (Fig. 8 *A*). For these samples, the excitation GP spectrum (as well as many other techniques) reveals the coexistence of separate domains (Fig. 1 *B*). However, we note that the GP histogram is not clearly bimodal. The higher GP values in the distribution (Fig. 8 *A*) are lower than those expected for a pure gel phase, indicating that more water can penetrate the DPPC phase. The lower GP values of the distribution histogram are higher than those expected for the pure DOPC phase, indicating that less water is present in the mixture sample. From the GP histogram we conclude that the domains of high GP are not simply domains of pure gel, in agreement with previous findings (Parasassi et al., 1993b). The image of this mixture (Fig. 7) shows disjoined regions of high and low GP, similar to the images of the pure DLPC and DOPC vesicles. In analogy with the analysis of the DLPC and DOPC vesicles, our interpretation model suggests that the domains (which are known to exist in this model) either are very small within a single layer, or each layer contains large domains, but we observe multiple layers in each pixel. The hypothesis of small (lateral) dimensions for these domains is in agreement with previous calculations based on spectroscopic observations. From time-resolved studies of laurdan spectral shift in vesicles composed of various relative concentrations of DLPC and DPPC

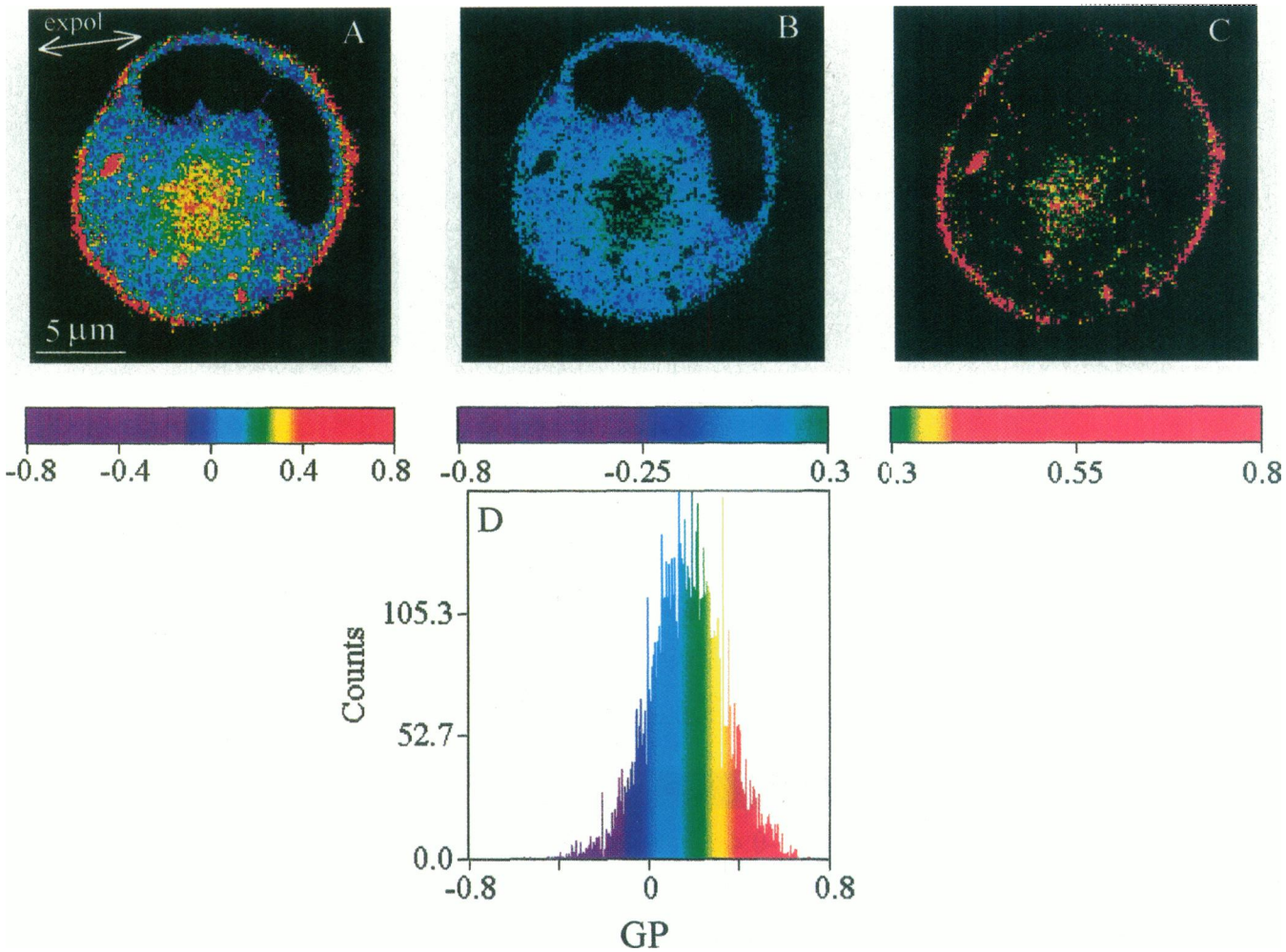

FIGURE 13 (*A*) GP images of OK cells labeled with laurdan obtained at room temperature (~20°C). The colors indicate different GP values following the reported scale. In *B* and *C* the low and high GP values are drawn, respectively, following the reported scales. (*D*) Distribution of the GP values. The image scale bar is reported in *A*, together with the direction of the excitation polarization.

(Parasassi et al., 1993b), the domains' linear dimensions were estimated to range between 2 nm and 5 nm, well below the resolution of the two-photon microscope (about 200 nm in the axial plane).

Cholesterol induces heterogeneity in the gel phase

The morphological and dynamic modifications induced by cholesterol on the pure and mixed phospholipid phases, as observed with the two-photon microscope, are quite impressive. Previous studies reported a strong modification of phospholipid phase properties in the presence of cholesterol (Ipsen et al., 1987, 1989; Vist and Davis, 1990; Mouritsen, 1991). Depending on their relative concentrations and on temperature, the phase properties of vesicles composed of binary mixtures of cholesterol and phospholipids have been described by the solid-ordered, liquid-disordered, and liquid-ordered phases. These phases account for the increase in translational and rotational motions of the phospholipids in the gel phase in the presence of cholesterol, and for their decrease in the liquid-crystalline phase (Mouritsen, 1991). In a few words, cholesterol renders the gel phase more fluid and the liquid-crystalline phase more solid. From our polarized microscopic images we can see that in DPPC vesicles, the presence of 30 mol% cholesterol does not induce an average disordering effect. The main component of the GP histogram (Fig. 8 *B*) moves to higher GP values, indicating that the bilayer is more ordered and that less water is present. Instead, we observe a smaller component in the GP distribution at low GP. However, the pixels corresponding to the lower values of the distribution are uniformly distributed in these vesicles (Fig. 9 *B*), maybe with a tendency to align along circles. According to our model interpretation, the GP domains corresponding to this part of the distribution must have dimensions similar to or larger than the pixel size. In this respect, the higher translational motion reported for the liquid-ordered phase can be due to this population of more fluid areas in the gel phase when cholesterol is present.

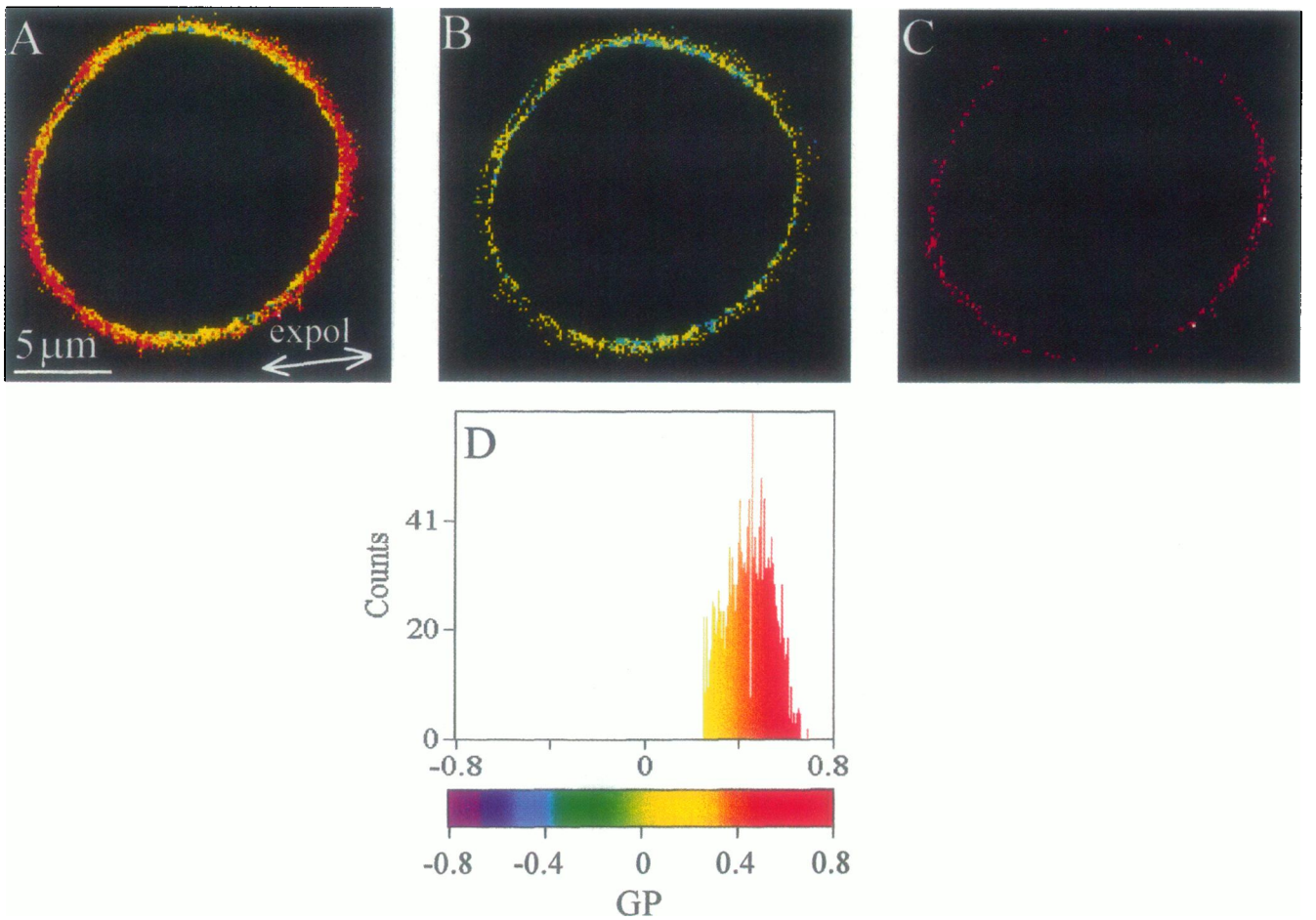

FIGURE 14 GP images of the plasma membrane of OK cells, isolated from Fig. 13 *A*. (*A*) The full image; (*B*) the low GP values; (*C*) the high GP values; (*D*) the GP value distribution. All colors follow the reported scale.

Cholesterol homogenizes the phases

The effect of the addition of 30 mol% cholesterol to the equimolar mixture of DOPC and DPPC on the emission (Fig. 2 *A*) and on the GP spectra (Fig. 2 *B*) is similar to that already reported for the equimolar mixture of DLPC and DPPC (Parasassi et al., 1994). In comparison with the same sample without cholesterol, the emission spectrum is blue shifted, and the wavelength dependence of the excitation GP spectrum has a negative slope. As discussed above, the characteristic behavior of the GP as a function of excitation wavelength has been used to discriminate between bilayers composed of coexisting domains of different phases and of homogeneous intermediate phase properties (Parasassi et al., 1993b). By adding cholesterol to phospholipid vesicles composed of equimolar concentrations of the two phases, the positive slope observed in the presence of coexisting domains was reported to progressively decrease, so that at cholesterol concentrations above 10–15 mol%, the excitation GP spectra show the wavelength dependence typical of a homogeneous liquid-crystalline phase (negative slope), although the absolute GP values are higher (Parasassi et al., 1994).

The microscopic GP images of the DOPC-DPPC vesicles with 30 mol% support this picture. The vesicles appear to be strongly polarized, with a relatively broad GP distribution (Fig. 8 *C*). The section of the vesicles in Fig. 10 is relatively close to the supporting quartz slide, so that the center of the section of the vesicle corresponds to regions in which laurdan molecules are aligned perpendicular to the excitation polarization direction. This part of the image (the center of the section) displays a relatively low GP, indicating that also in this sample it is possible to preferentially excite molecules with lower GP. It is noteworthy that the image obtained with nonpolarized excitation (but the light is always polarized in a plane perpendicular to the direction of light propagation) still shows a region of low GP at the center of the vesicle section, because in this section the plane of light polarization is perpendicular to the laurdan transition dipole moment. There is still an apparent large GP distribution, as judged by the GP histogram (Fig. 8 *D*).

In RBCs, GP domains are comparable to the microscope resolution

RBC images display only a section of the cell membrane. We deduce from the characteristic polarization pattern that laurdan molecules have their transition dipole moment

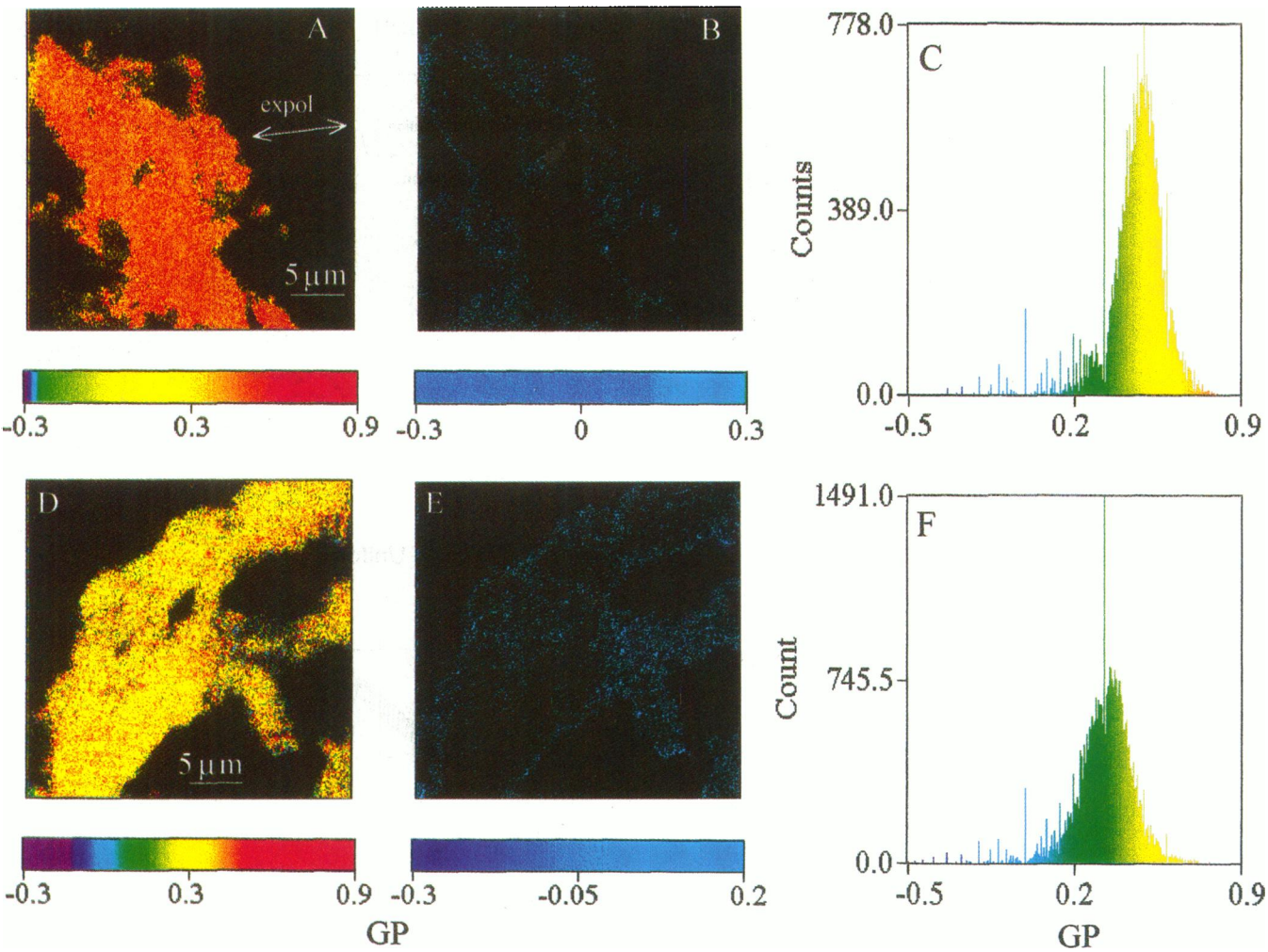

FIGURE 15 GP images (*A*, *B*, *D* and *E*) and histograms (*C* and *F*) of purified rat renal brush border (*A*, *B*, and *C*) and basolateral membranes (*D*, *E*, and *F*) labeled with laurdan at room temperature (~20°C). The colors indicate different GP values following the reported scales. The image scale bar is reported in *A*, together with the direction of the excitation polarization. In *B* and *E* only low GP values are drawn, using the colors indicated in the corresponding scales. Polarized excitation light has been used; the direction of polarization is ~10° with respect to the horizontal.

pointing toward the center of the cell, in accord with the vesicle studies. The GP distribution is relatively broad. If we plot pixels with relatively high GP (>0.5), they appear in the equatorial part of the membrane (Fig. 12 *C*). If we plot pixels with relatively low GP (<0.3) instead, they appear to be equally distributed along the membrane (Fig. 12 *B*). Following our model interpretation, this cell membrane should have domains of sizes comparable to the microscope resolution.

In OK cells, GP domains are smaller than the microscope resolution

For the images of OK cells, the pattern is not as clear as with the RBCs. The high GP regions are mainly in the equatorial plane. However, the low GP image (Fig. 13 *B*), which appears to be uniformly populated all over the cell section and along the plasma membrane, is more difficult to interpret. There is a large contribution from laurdan in internal membranes, and it is difficult to assign pixels of low GP to the external membrane only. Therefore we masked the cell interior to better visualize the regions of the plasma membrane only. Fig. 14, *B* and *C*, shows the low and high GP images of the masked cells. These images clearly display the characteristic distribution due to the polarized excitation light, and the high and low GP regions are almost completely disjoined. According to our model interpretation for this external membrane, the size of the GP domains is smaller than the microscope resolution.

In BBM and BLM membranes, apparent GP domains are relatively large

BBM and BLM membranes are known to possess a different lipid composition, including cholesterol content, that leads to different average GP values, higher in the BBM membranes and lower in the BLM membranes. The two-photon excitation GP images of these membranes agree

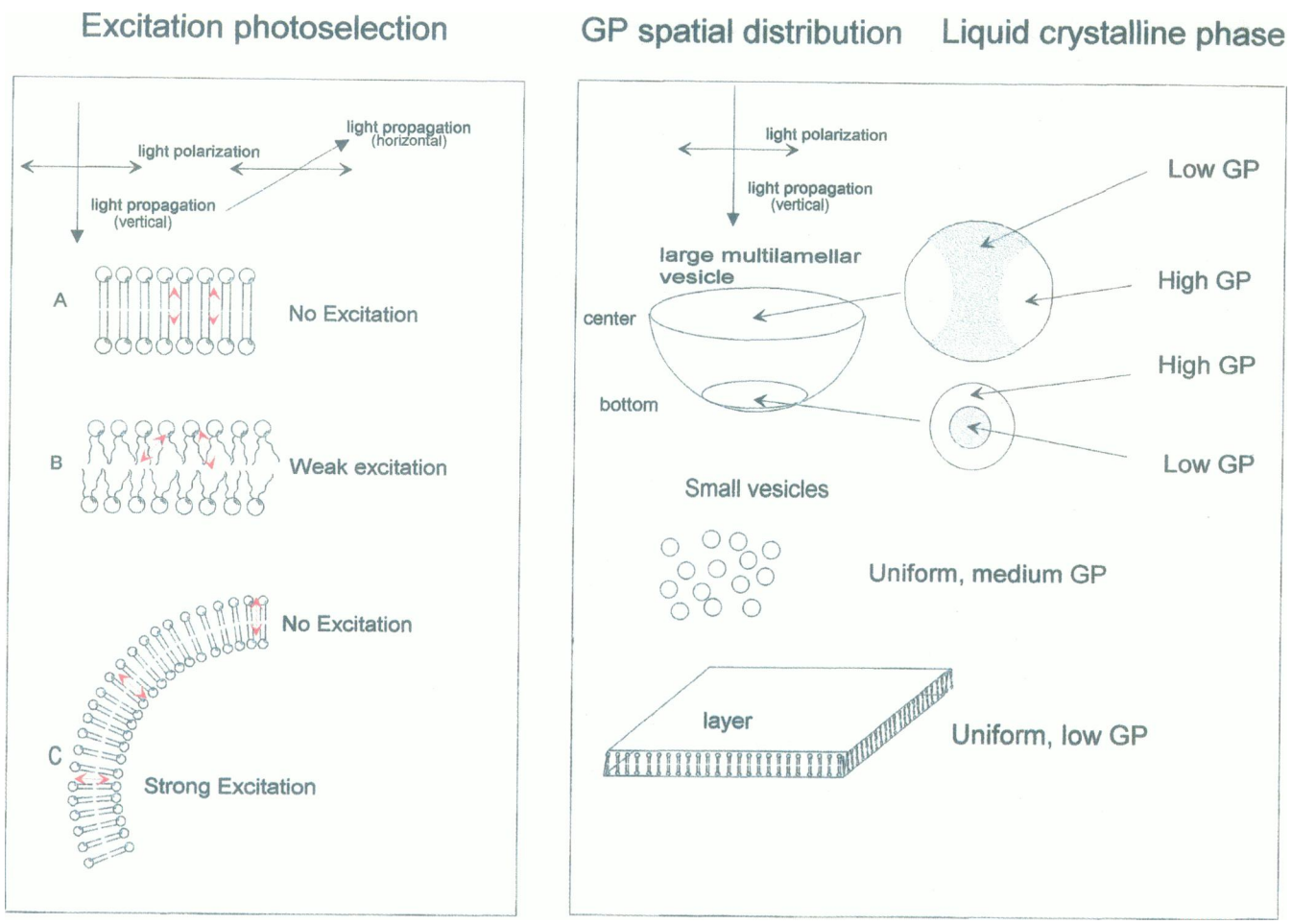

FIGURE 16 Schematic representation of excitation photoselection and GP spatial distribution. i) Excitation photoselection. In the upper part, two different excitation geometries cause the same photoselection effect. (*A*) No excitation is obtained, because the direction of the transition dipole moment of the laurdan molecule is perpendicular to the excitation polarization. (*B*) There is weak excitation of those molecules that have a projection of the transition dipole moment along the membrane surface. (*C*) As we travel along the circumference of the membrane, the direction of the transition dipole moment changes from the polar regions, where there is no excitation, to the equatorial regions, where strong excitation occurs. ii) GP spatial distribution. This panel only shows the GP patter expected in the liquid crystalline phase. The patterns are obtained by using the photoselection rules and the presumed correlation between the size of the vesicle cavity and the GP value.

with these previous findings (Levi et al., 1987, 1989, 1990). Average higher GP values can be observed in the BBM images. Nevertheless, the images from these samples also show a complex texture of small domains with different GP values, and the GP histograms show a relatively broad distribution. Because of the poor local orientation of these membrane preparations, the polarization effect is not evident. Nevertheless, when these images are sectioned for selected windows of low or high GP values, we observe structures (for example, the membrane borders in Fig. 15) clearly indicating that the GP values reflect spatially distinct domains. The lower GP values of these border areas can be explained by the more fragile, fluid, membrane breaking points. We must be cautious in interpreting the GP images of these membrane preparations. Our interpretation model is based on an assumption about the orientation of the membranes. Whereas this assumption may be valid for multilamellar vesicles, the actual structure of our BLM and BBM membrane preparation is unknown. A change in local orientation may result in a change in the apparent GP value, only because different orientations select different environments. Whatever the interpretation, there must be an intrinsic GP heterogeneity, either at the submicroscopic level (in this case the regions of different GP may simply correspond to regions of different lipid orientation) or in regions resolvable by the microscope (in which case the GP domains shown in the image correspond to real "fluidity" domains).

We thank Dr. Peter So for the red blood cell preparations and images.

This work was supported by the National Institutes of Health (RR03155 to EG and WMY), by the CNR (to TP), and by Department of Veterans Affairs Merit Review grants (to ML).

REFERENCES

Aloia, R. C., H. R. Tian, and F. C. Jansen. 1993. Lipid composition and fluidity of the human immunodeficiency virus envelope and host cell plasma membrane. *Proc. Natl. Acad. Sci. USA.* 90:5181–5185.

Arar, M., M. Baum, J. Biber, H. Murer, and M. Levi. 1995. Epidermal growth factor inhibits Na-P_i cotransport and mRNA in OK cell. *Am. J. Physiol.* 268:F309–F314.

Borle, F., and J. Seelig. 1983. Hydration of *Escherichia coli* lipids: deuterium T_1 relaxation time studies of phosphatidylglycerol, phosphatidylethanolamine and phosphatidylcholine. *Biochim. Biophys. Acta.* 735: 131–136.

Chiu, S. W., M. Clark, V. Balaji, S. Subramaniam, L. H. Scott, and E. Jakobsson. 1995. Incorporation of surface tension into molecular dunamics simulation of an interface: a fluid phase lipid bilayer membrane. *Biophys. J.* 69:1230–1245.

Chong, P. L. 1994. Evidence for regular distributions of sterols in liquid-crystalline phosphatidylcholine bilayers. *Proc. Natl. Acad. Sci. USA.* 91:10069–10073.

Chong, P. L., D. Tang, and I. P. Sugar. 1994. Exploration of physical principles underlying lipid regular distribution: effects of pressure, temperature and radius of curvature on E/M dips in pyrene-labeled PC/DMPC binary mixtures. *Biophys. J.* 66:2029–2038.

Grant, C. W. M. 1983. Lateral phase separations and the cell membrane. *In* Membrane Fluidity in Biology, Vol. 2. R. C. Aloia, editor. Academic Press, New York. 131–150.

Ipsen, J. H., G. Karlstron, O. G. Mouritsen, H. Wennerstrom, and M. H. Zuckermann. 1987. Phase equilibria in the phosphatidylcholine-cholesterol system. *Biochim. Biophys. Acta.* 905:162–172.

Ipsen, J. H., O. G. Mouritsen, and M. J. Zuckermann. 1989. Theory of thermal anomalies in the specific heat of lipid bilayers. *Biophys. J.* 56:661–667.

Levi, M., B. M. Baird, and P. V. Wilson. 1990. Cholesterol modulates rat renal brush border membrane phosphate transport. *J. Clin. Invest.* 85: 231–237.

Levi, M., D. M. Jameson, and B. W. van der Meer. 1989. Role of BBM lipid composition and fluidity in impaired renal P_i transport in aged rat. *Am. J. Physiol.* 256:F85–F94.

Levi, M., B. A. Molitoris, T. J. Burke, R. W. Schrier, and F. R. Simon. 1987. Effects of vitamin D-induced hypercalcemia on rat renal cortical brush border and basolateral membranes and mitochondria. *Am. J. Physiol.* 252:F267–275.

Maresca, B., and A. R. Cossins. 1993. Cell physiology: fatty feedback and fluidity. *Nature.* 365:606–607.

Molitoris, B. A., and F. R. Simon. 1985. Renal cortical brush-border and basolateral membranes: cholesterol and phospholipid composition and relative turnover. *J. Membr. Biol.* 83:207–215.

Mouritsen, O. G. 1991. Theoretical models of phospholipid phase transitions. *Chem. Phys. Lipids.* 57:179–194.

Parasassi, T., G. De Stasio, A. d'Ubaldo, and G. Gratton. 1990. Phase fluctuation in phospholipid membranes revealed by laurdan fluorescence. *Biophys. J.* 57:1179–1186.

Parasassi, T., M. Di Stefano, G. Loiero, G. Ravagnan, and E. Gratton. 1994. Influence of cholesterol on phospholipid bilayers phase domains as detected by laurdan fluorescence. *Biophys. J.* 66:120–132.

Parasassi, T., A. M. Giusti, M. Raimondi, and E. Gratton. 1995. Abrupt modification of phospholipid bilayer properties at critical cholesterol concentrations. *Biophys. J.* 68:1895–1902.

Parasassi, T., and E. Gratton. 1995. Membrane lipid domains and dynamics as detected by laurdan fluorescence. *J. Fluorescence.* 5:59–69.

Parasassi, T., M. Raimondi, G. Ravagnan, and E. Gratton. 1993a. Absence of lipid gel phase domains in seven mammalian cell lines and in four primary cell types. *Biochim. Biophys. Acta.* 1153:143–154.

Parasassi, T., G. Ravagnan, R. M. Rusch, and E. Gratton. 1993b. Modulation and dynamics of phase properties in phospholipid mixtures detected by laurdan fluorescence. *Photochem. Photobiol.* 57:403–410.

Rodgers, W., and M. Glaser. 1991. Characterization of lipid domains in erythrocyte membranes. *Proc. Natl. Acad. Sci. USA.* 88:1364–1368.

Sankaram, M. B., and T. E. Thompson. 1990. Modulation of phospholipid acyl chain order by cholesterol. A solid-state ^2H nuclear magnetic resonance study. *Biochemistry.* 29:10676–10684.

So, P. T. C., T. French, W. M. Yu, K. M. Berland, C. Y. Dong, and E. Gratton. 1995. Time-resolved microscopy using two-photon excitation. *Bioimaging.* 3:49–63.

So, P. T. C., T. French, W. M. Yu, K. M. Berland, C. Y. Dong, and E. Gratton. 1996. Two-photon fluorescence microscopy: time-resolved and intensity imaging in fluorescence imaging spectroscopy and microscopy. X. F. Wang and B. Herman, editors. Chemical Analysis Series, Vol. 137. John Wiley and Sons, New York. 351–374.

Tang, D., and P. L. Chong. 1992. E/M dips. Evidence for lipids regularly distributed into hexagonal super-lattices in pyrene-PC/DMPC binary mixtures at specific concentrations. *Biophys. J.* 64:399–412.

Virtanen, J. A., M. Ruonala, M. Vauhkonen, and P. Somerharju. 1995. Lateral organization of liquid-crystalline cholesterol-dimyristoylphosphatidylcholine bilayers. Evidence for domains with hexagonal and centered rectangular cholesterol superlattices. *Biochemistry.* 34: 11568–11581.

Virtanen, J. A., P. Somerharju, and P. K. J. Kinnunen. 1988. Prediction of patterns for the regular distribution of soluted guest molecules in liquid crystalline phospholipid membranes. *J. Mol. Electron.* 4:233–236.

Vist, M. R., and J. D. Davis. 1990. Phase equilibria of cholesterol dipalmitoyl-phosphatidylcholine mixtures; ^2H nuclear magnetic resonance and differential scanning calorimetry. *Biochemistry.* 29:451–464.

Yu, W., P. T. C. So, T. French, and E. Gratton. 1996. Fluorescence generalized polarization of cell membranes: a two-photon scanning microscopy approach. *Biophys. J.* 70:626–636.